Shell-model molecular dynamics simulation of superionic conduction in CaF_2

1993 J. Phys.: Condens. Matter 5 1019

(http://iopscience.iop.org/0953-8984/5/8/005)

J. Phys.: Condens. Matter 5 (1993) 1019–1030. Printed in the UK

Shell-model molecular dynamics simulation of superionic conduction in CaF_2

P J D Lindan and M J Gillan
Physics Department, Keele University, Keele, Staffordshire ST5 5BG, UK

Received 23 July 1992, in final form 18 November 1992

Abstract. We have developed a new code for performing molecular dynamics simulations of ionic materials, in which electronic polarization is included via the shell model. Key features of the method are the use of the conjugate-gradients technique for relaxing the shells at each step, and a new device for ensuring energy conservation. The new code is used to study superionic conduction in CaF_2, which has previously been studied by conventional rigid-ion molecular dynamics. For both static and dynamic quantities, the modifications caused by explicit inclusion of electronic polarizability are remarkably small.

1. Introduction

The purpose of this paper is twofold. Firstly, we report on an improved shell-model molecular dynamics (MD) method for performing atomistic simulations of ionic materials with full inclusion of the electronic polarizability of the ions. Secondly, we present the results of simulations of the superionic conductor CaF_2 performed using the method. The aim of these simulations is to examine the influence of explicit inclusion of polarizability on static and dynamic quantities in superionic CaF_2.

Molecular dynamics simulation has played a key role in the theoretical study of ionic materials, and has been used to investigate the nature of the ionic disorder and the dynamics of the conduction process in a wide range of superionic conductors, including fluorites such as CaF_2 (see e.g. Rahman 1976, Dixon and Gillan 1978, Parrinello *et al* 1983, Wolf *et al* 1984, Gillan 1986, 1989, Smith and Gillan 1992). Almost all this work has been done using rigid-ion models for the interactions between the ions. In the rigid-ion approximation, the electronic polarizability of the ions is ignored, and the total energy U of the system (excluding kinetic energy of the ions) is generally written as a sum of pair interactions:

$$U = \frac{1}{2}\sum_{\alpha,\beta}\sum_{ij} V_{\alpha\beta}(|\mathbf{r}_{\alpha i} - \mathbf{r}_{\beta j}|) \tag{1}$$

where α, β represent the ionic species, and $\mathbf{r}_{\alpha i}$ is the position of ion i of species α. The pair potential is often assumed to have the Born–Mayer–Huggins form (see e.g. Catlow and Mackrodt 1982):

$$V_{\alpha\beta}(r) = z_\alpha z_\beta e^2/r + A_{\alpha\beta}\exp(-r/\rho_{\alpha\beta}) - C_{\alpha\beta}/r^6 \tag{2}$$

0953-8984/93/081019+12$07.50

where z_α is the charge on ions of species α in units of the elementary charge e and the second and third terms on the righthand side represent the overlap-repulsion and dispersion energies respectively. The rigid-ion approximation has two serious limitations. The first is that is predicts a high-frequency dielectric constant ϵ_∞ equal to unity. In real ionic materials ϵ_∞ is usually at least two, and in oxides values of over five are quite common. This mis-representation of the dielectric properties means that lattice vibrational frequencies are inevitably wrong. The second limitation is methodological. Most work on the static structure and the defect and surface energetics of ionic materials is based on a shell-model representation of the interactions, in which electronic polarizability is fully included, and dielectric properties are correctly described (Catlow and Mackrodt 1982, Harding 1990). The almost universal use of rigid-ion models for dynamic simulations and shell-models for static simulations is currently preventing a unified approach.

One of the aims of the present work is to show that shell-model MD simulation can be performed straightforwardly and routinely, and we have therefore sought to develop a shell-model code which works efficiently for any ionic system. Shell-model MD is, of course, far from new. Shell-model simulations of molten salts were performed many years ago by Jacucci *et al* (1976) and by Sangster and Dixon (1976). Unfortunately, the technique has not been widely used and has acquired a reputation for being difficult to apply and extremely demanding on computer resources. Important recent work using the technique has, nonetheless, been reported (Board and Elliott 1989, O'Sullivan and Madden 1991). We believe that the greatly increased computer power that is now readily available makes the present re-examination of the shell-model MD technique timely.

The technical difficulties in shell-model simulation stem from the fact that the shells have zero mass. This means that at every instant during the simulation the net force acting on every shell must vanish. Like earlier workers (Jacucci *et al* 1976, Sangster and Dixon 1976), we achieve this by iteratively relaxing all the shells at each MD time-step. This is done by the conjugate-gradients technique (Fletcher 1980, Press *et al* 1986), which we expect to be more powerful and general than the steepest-descent method used in previous work. The iterative relaxation method has generally been found to lead to a drift in the total energy (Sangster and Dixon 1976). We show that this problem can be overcome by a simple device in which the initial positions of the shells at each time step are adjusted in a suitable way.

The simulation technique is described in section 2. Initial tests of the technique on a shell-model for CaF_2 are summarized in section 3. This is followed in section 4 by a description of the simulations we have performed on CaF_2 in the superionic state. These yield results for the radial distribution functions, the spatial probability distributions of the ions, and the fluorine diffusion coefficient, which we compare with the results of rigid-ion simulations. Our conclusions are summarized in the final section.

2. Techniques

2.1. Overview

In the shell model (Dick and Overhauser 1958), each ion consists of a core and a shell, which carry charges and are coupled to each other by a harmonic spring. All the mass of each ion is in its core, so that the shell is massless. The core and shell on each ion

interact with the cores and shells on all other ions via the Coulomb interaction. There are also short-range interactions between the ions, which are usually taken to act only between shells. Because the shells have no mass, they respond instantaneously to the motion of the cores: for any set of core positions, the positions of the shells are such that the force on every shell is zero. The energy is thus a minimum with respect to the shell positions. This represents the physical fact that the system is always in the ground state with respect to the electronic degrees of freedom.

The motion of the cores is governed by the usual Newtonian equation for motion, for which we need the forces acting on the cores. For a given set of core positions, these forces must be calculated with the shells fully relaxed. A single dynamical step in the simulation therefore consists of (i) calculation of the forces on all cores with all shells relaxed; (ii) updating of core positions using these forces, which we perform by Verlet's algorithm; (iii) relaxation of all shells for the new core positions, ready for the next step. Shell relaxation at each step must be performed iteratively.

2.2. Shell relaxation

Relaxation of the shells at each time step involves a search in the multi-dimensional space of shell configurations. In previous work (Sangster and Dixon 1976), this search has generally been performed by the steepest-descents method. Although this has been made to work for particular cases, the method as a general technique suffers from serious weaknesses, and is unlikely to yield the robustness and efficiency we seek in the present work. We base our method on the more powerful conjugate-gradients technique (for general descriptions of the method, see Fletcher 1980, Press *et al* 1986).

For a given set of core positions, let $\boldsymbol{u}_i$ denote the position of the shell of ion i relative to its core. At the kth step of iterative relaxation, let the shell positions be $\boldsymbol{u}_i^{(k)}$ and the forces on the shells be $\boldsymbol{f}_i^{(k)}$. In taking the next relaxation step to shell positions $\boldsymbol{u}_i^{(k+1)}$, we make displacements along a search direction specified by vectors $\boldsymbol{s}_i^{(k)}$:

$$\boldsymbol{u}_i^{(k+1)} = \boldsymbol{u}_i^{(k)} + \lambda \boldsymbol{s}_i^{(k)} \tag{3}$$

where the variable λ specifying the size of the step is to be adjusted so that the energy is minimised for this search direction. In the steepest-descents method, the shells would be made to move in the direction of the forces, so that one takes $\boldsymbol{s}_i^{(k)} = \boldsymbol{f}_i^{(k)}$. Even in relatively trivial cases, this method requires an infinite number of line searches. The key feature of the conjugate-gradients method is that information accumulated during the relaxation process is used to construct more intelligent search directions. Specifically, the present search vector $\boldsymbol{s}_i^{(k)}$ depends both on the present force $\boldsymbol{f}_i^{(k)}$ and the previous search vector $\boldsymbol{s}_i^{(k-1)}$:

$$\boldsymbol{s}_i^{(k)} = \boldsymbol{f}_i^{(k)} + \beta^{(k)} \boldsymbol{s}_I^{(k-1)}. \tag{4}$$

In the present work, we employ the conventional choice for $\beta^{(k)}$, which is

$$\beta^{(k)} = \sum_i |\boldsymbol{f}_i^{(k)}|^2 \Big/ \sum_i |\boldsymbol{f}_i^{(k-1)}|^2. \tag{5}$$

The justification for this choice, and the guarantees it provides about the manner of convergence to the minimum are described in the literature (Fletcher 1980, Press *et al* 1986).

A procedure also has to be adopted for minimising along each search direction. In designing this, we assume that the energy is nearly quadratic in u_i. This will be true provided the shells are never too far from the minimum, which can be ensured by a appropriate choice of time step. Our procedure works as follows.

Starting from given shell positions, we make a step along the search direction. In choosing an appropriate value of λ, we use the value of $\partial E/\partial\lambda$ at $\lambda = 0$, which is

$$\partial E/\partial\lambda|_{\lambda=0} = -\sum_i \boldsymbol{f}_i^{(k)} \cdot \boldsymbol{s}_i^{(k)}. \tag{6}$$

The value of λ is then chosen so that we would arrive at the minimum along the search direction if the curvature $\partial^2 E/\partial\lambda^2$ was determined entirely by the springs, so that

$$\partial^2 E/\partial\lambda^2 = \sum_i k_i |\boldsymbol{s}_i^{(k)}|^2. \tag{7}$$

The appropriate λ, which we denote by λ_1, is thus given by

$$\lambda_1 = \sum_i \boldsymbol{f}_i^{(k)} \cdot \boldsymbol{s}_i^{(k)} \Big/ \sum_i k_i |\boldsymbol{s}_i^{(k)}|^2. \tag{8}$$

Let the values of E before and after displacements be called E_0 and E_1, corresponding to $\lambda = 0$ and λ_1. We now fit a parabola to E_0, E_1 and $\partial E/\partial\lambda$ at $\lambda = 0$ to obtain an improved estimate λ_2 for λ at the minimum, and we recalculate the energy at this point—call it E_2. Now if the lower of E_1 and E_2 is lower than E_0 (which is almost always the case) then we accept the corresponding shell positions $\boldsymbol{u}_i^{(k+1)}$ as the start of a search in a new direction.

Occasionally, E_1 and E_2 both fail to be lower than E_0 for the very first search direction, because the initial guess for the $\boldsymbol{u}_i$ is so far from the minimum that the quadratic approximation breaks down. In this case, we take the next value λ_3 of λ to be a fixed fraction σ of λ_2; the value of σ always remains the same, and we generally take it equal to 0.1. If the energy E_3 at $\lambda = \lambda_3$ is still greater than E_0, we successively reduce λ by a factor of two until the energy falls below E_0, whereupon the search in the given direction is terminated. Near the end of the minimization procedure, E_1 and E_2 can also both lie above E_0 if we are so close to the minimum that rounding errors are preventing progress. In this case, a single further attempt is made to reduce the energy, by reducing λ_2 by a fixed fraction. If this achieves nothing, the search in the given direction is terminated.

The entire minimization process for a given time step is terminated when we arrive at a search direction in which no progress proves to be possible. As a convenient test of performance, we monitor the progress of minimization at each time step through the RMS shell force $\bar{f}$ defined as

$$\bar{f} = \left(N^{-1} \sum_{i=1}^{N} |\boldsymbol{f}_i|^2 \right)^{1/2} \tag{9}$$

where N is the number of ions in the system. Results of such tests will be described in section 3.

The efficiency of conjugate-gradients minimization of the shells is further improved by preconditioning, i.e. rescaling of the variables. The motivation for this can be understood by considering the simulation where the variation of energy with shell

positions is dominated by the harmonic springs; this happens for strong springs, i.e. very unpolarizable ions. For fixed core positions, the energy can be written approximately as

$$E = E_0 + \frac{1}{2}\sum_i k_i |\boldsymbol{u}_i - \boldsymbol{u}_i^0|^2 \tag{10}$$

where $\boldsymbol{u}_i^0$ are the equilibrium shell positions and E_0 is the minimum energy. We have two or more species of ions, so that the spring constants k_i are not all the same. The forces on the shells are given by

$$\boldsymbol{f}_i = -k_i\left(\boldsymbol{i}_i - \boldsymbol{u}_i^0\right) \tag{11}$$

so that the displacement needed to take us directly to the minimum is

$$\boldsymbol{u}_i^0 - \boldsymbol{u}_i = \boldsymbol{f}_i / k_i. \tag{12}$$

Note that, even in this simple case, the steepest-descents method is inefficient, since it makes the displacements proportional to $\boldsymbol{f}_i$ instead of $\boldsymbol{f}_i/k_i$; the method would need an infinite sequence of searches to attain the minimum. Even the conjugate gradients method needs a number of search directions equal to the number of different spring constants. This can be reduced to one search if we rescale the variables by working with $\tilde{\boldsymbol{u}}_i = k_i^{1/2}\boldsymbol{u}_i$, so that

$$E = E_0 + \frac{1}{2}\sum_i |\tilde{\boldsymbol{u}}_i - \tilde{\boldsymbol{u}}_i^0|^2 \tag{13}$$

with the associated forces $\tilde{\boldsymbol{f}}_i$ given by

$$\tilde{\boldsymbol{f}}_i = -\partial E / \partial \tilde{\boldsymbol{u}}_i. \tag{14}$$

This simple preconditioning is incorporated in our method.

Finally, we have to decide how to initiate the minimization process at each step: we need a set of initial shell positions $\boldsymbol{u}_i^{(0)}$. The simplest procedure, which we adopt as a point of reference, is to take the initial shell–core displacements at the new time step to be equal to the fully relaxed shell–core displacements at the previous step, as has been done in earlier work (Sangster and Dixon 1976).

2.3. Energy conservation

The conjugate-gradients procedure is robust and automatic, but the method as described above does not ensure satisfactory energy conservation. Even with energy minimization at each time step performed to high accuracy, there is a continual downward drift in energy and the temperature steadily decreases. This is a problem which has also beset previous shell-model MD methods (see e.g. Sangster and Dixon 1976). Our tests show that the problem arises from the initial conditions used in our iterative relaxation. The initial guess that $\boldsymbol{u}_i$ is the same as in the relaxed configuration of the previous step has the effect of making the calculated relaxed positions of the shells lag slightly behind where they should be. This is a rather subtle point, and it is worth stressing that the problem arises only because the minimization is imperfect. If the shells were relaxed to their exact zero-force positions, the initial guess would be irrelevant. The situation seems to be that the bias in the initial guess leads to a bias in the calculated relaxed positions, because the minimization if imperfect.

We have adopted two methods to overcome the problem of energy drift. The first is simply a 'fix': we rescale the velocities at each time step so as to ensure that the total energy at each step is precisely the same as at the previous step. A gentler and more stable variant of this is to rescale the velocities so as to restore only a fraction of the energy change since the previous step. Our tests show that this produces a completely stable method, but there is an undesirable side effect, which is that after long equilibration the temperatures of the different ionic species can be noticeably different. The effect is small in test calculations on CaF_2, but is more significant in trials we have made on UO_2. For this reason, we have not adopted enforcement of energy conservation as a general method, and it is not the method used in the simulations on CaF_2 reported later.

Our device for eliminating energy drift is based on the observation that the drift is *downwards*. This means that on the average the shells are producing a spurious drag force on the cores: the error in the force on the cores is, on the average, in the opposite direction to the velocity of the cores. Since we believe that the bias comes from our choice of initial shell positions at each step, our solution is to modify this choice. Instead of always setting the initial shell–core displacement $\boldsymbol{u}_i^{(0)}$ at the present step t equal to the previous fully relaxed displacement $\boldsymbol{u}_i^{(\infty)}$, we set $\boldsymbol{u}_i^{(0)}$ in this way only at alternate steps. At the other steps, we add onto the initial displacement an increment proportional to the velocity of the core, or equivalently to the displacement of the core in that step. In other words, we take

$$\boldsymbol{u}_i^{(0)}(t) = \boldsymbol{u}_i^{\infty}(t - \Delta t) + \alpha[\boldsymbol{r}_i(t) - \boldsymbol{r}_i(t - \Delta t)]. \tag{15}$$

The parameter α is at our disposal, and needs to be chosen appropriately for each system under given thermodynamic conditions. However, the choice of α turns out in practice not to be critical, and provided α is large enough, the downward drift of energy is eliminated. Perhaps surprisingly, if we make α very large there is no resultant upward drift of energy, though more conjugate-gradients iterations are inevitably required.

2.4. Miscellaneous details

Apart from our incorporation of the ionic core–shell structure, our code uses fairly standard MD techniques. The usual periodic boundary conditions (cubic in the present case) are employed, and the code is designed to run at constant volume as well as constant energy. The Coulomb energy and forces are handled by the Ewald technique.

3. Potentials and tests

As a first application of our shell-model MD technique, we have chosen to study superionic CaF_2, for a number of reasons. Firstly, the material has already been extensively modelled by rigid-ion MD simulation (Rahman 1976, Dixon and Gillan 1978, 1980, Gillan 1986, Evangelakis and Pontikis 1989, 1991, Gillan 1989, Lindan and Gillan 1991), which provides a base-line for comparison. Secondly, well tested shell-model potentials are readily available, which are known to reproduce accurately the vibrational and defect properties of the real material. Thirdly, superionic conduction in CaF_2 has been well characterized experimentally.

Our simulations are based on the shell-model potential by Catlow and Norgett (1973), which treats both cations and anions as polarizable. The ions carry full ionic

charges, and the short-range interaction between ionic shells is modelled by a Born–Mayer–Huggins potential (equation (2)). The rigid-ion model of CaF_2 with which we shall make comparisons is that developed by Dixon and Gillan (1980), and used in simulations by Gillan (1986, 1989), by Brass (1989), by Evangelakis and Pontikis (1989, 1991) and by Lindan and Gillan (1991). We have made harmonic calculations to study how well the rigid-ion and shell-model potentials reproduce experimental results for the phonon dispersion relations (Elcombe and Pryor 1970). The rigid-ion model gives a reasonable semi-quantitative account of the frequencies, but the shell model brings a considerable improvement, particularly in respect of the optic frequencies. The longitudinal optic frequency in particular is poorly predicted by the rigid-ion model, being 20% too high in the zone centre.

As a simple technical test of our shell-model MD code, we have checked that it correctly reproduces the shell-model harmonic frequencies. We have done this by taking perfect-crystal initial conditions in which each ion is given a very small initial velocity chosen so that the crystal vibrates in a single mode. This has been done for a number of modes at the zone centre and the zone boundary; the dynamic code produces the correct frequencies to within 1% in almost all cases.

Tests have also been made to discover the time step needed for satisfactory energy conservation, the accuracy of energy conservation, the number of relaxation steps needed within each time step etc. These tests have been done on systems of both 96 and 324 ions; the results of these tests were very similar for the two sizes of system. We find that our shell-model MD code works satisfactorily with time steps very similar to those normally used in rigid-ion simulations. For the work reported in the next section, a time step of 5.0 fs was used. In a typical simulation run, an average of ten line searches are made within every time step, the residual forces on the shells being generally no more than 10^{-3} of the RMS force on the cores.

As an indication of the speed of the code, we note that when run on a Hewlett–Packard 730 workstation, the 96-ion and 324-ion systems require an average of 4.2 and 25.0 CPU seconds per time step.

4. Shell-model simulations of CaF_2

We have used our shell-model MD code to perform simulations of CaF_2 in the superionic state at four different temperatures. It is known from a large body of experimental data that CaF_2 shows a diffuse transition from the normal to the superionic state at about 1420 K, this temperature being marked by a peak in the specific heat. Electrical conductivity and neutron-scattering measurements (Derrington *et al* 1975, Hayes and Hutchings 1989) as well as rigid-ion MD simulations (Dixon and Gillan 1980, Gillan 1986, 1989), have shown that at around this temperature there is a strong increase in the degree of disorder on the fluorine sublattice and the fluorine diffusion coefficient attains liquid-like values. This transition temperature is about $\frac{4}{5}$ of the melting temperature (CaF_2 melts at 1690 K).

In order to cover the superionic regime, we have made simulations at temperatures of 1500, 1600, 1670 and 1700 K. The simulations were performed on a system of 324 ions (108 Ca^{2+} and 216 F^-) interacting via the shell-model potential described in section 3. The molar volume at each temperature was taken to have its experimental value (Harding 1989). The total duration of each simulation, after 5 ps of equilibration, was 37.5 ps.

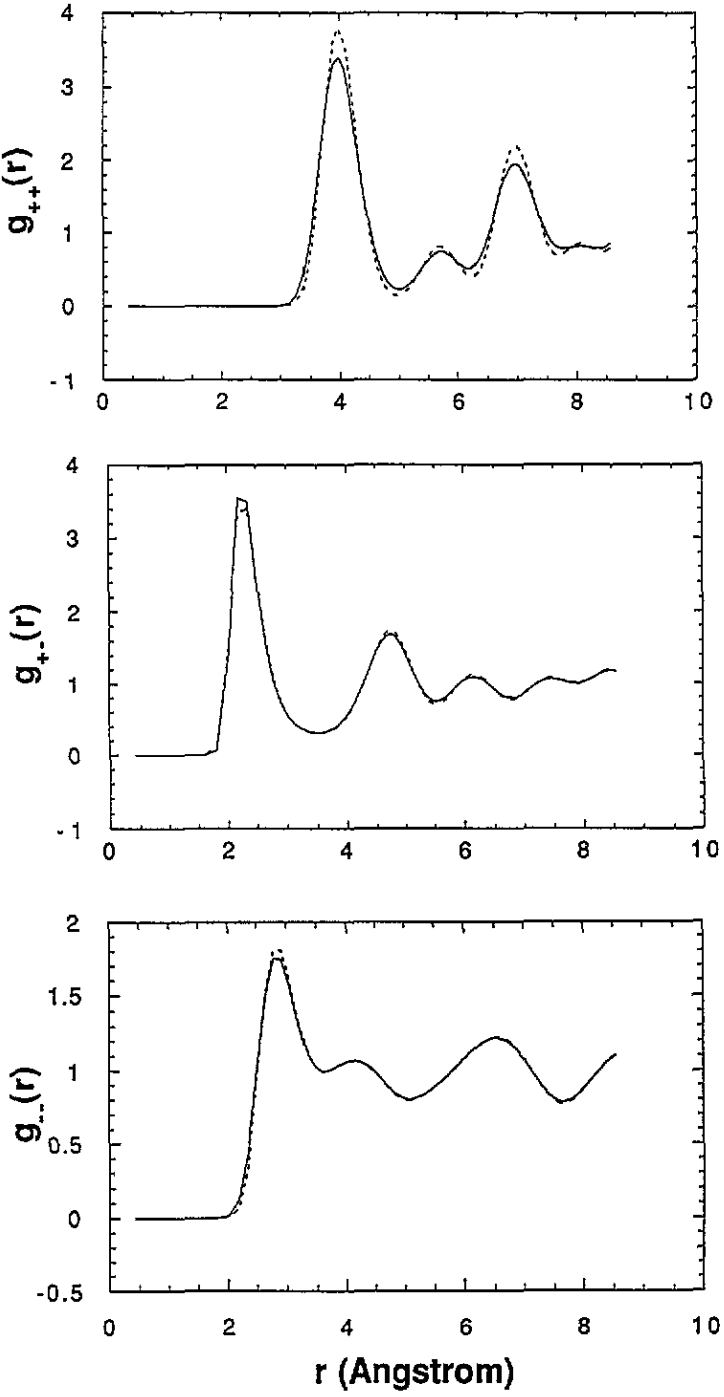

Figure 1. Radial distribution functions $g_{\alpha\beta}(r)$ from shell-model simulations (full curve) compared with rigid-ion results (broken curve). In both cases, simulations are for a system of 324 ions at a molar volume of 28.06 cm^3 and a temperature of 1670 K.

4.1. Radial distribution functions

We study the disorder in the system first through the radial distribution functions $g_{\alpha\beta}(r)$. Results for $g_{\alpha\beta}(r)$ at T = 1670 K re shown in figure 1, in comparison with rigid-ion results at the same temperature. As found in previous simulation work, the cation–cation and cation–anion function show strongly marked structure, typical of a high-temperature solid, while the anion–anion function has the weak structure characteristic of a liquid. The rigid-ion and shell-model results are in remarkably close agreement, though comparison of the cation–cation function $g_{++}(r)$ indicates that the cations vibrate with larger amplitudes in the shell-model system. Overall, however, the static structure in the superionic state is very little affected by the explicit inclusion of polarizability.

4.2. Single-particle density

A second useful method of studying the disorder is through the single-particle distribution functions $\rho_\alpha(r)$, defined as the probability density for finding an ion of type α at position r. We have calculated these quantities as described at Walker *et al* (1982): the simulation box is covered by a fine cubic grid, and the $\rho_\alpha(r)$ are accumulated as a three-dimensional histogram, with full use of symmetry to improve the statistics. Results for the anion distribution function $\rho_-(r)$ at 1670 K are shown in figure 2; for comparison, results are also shown for the rigid-ion system at the same temperature.

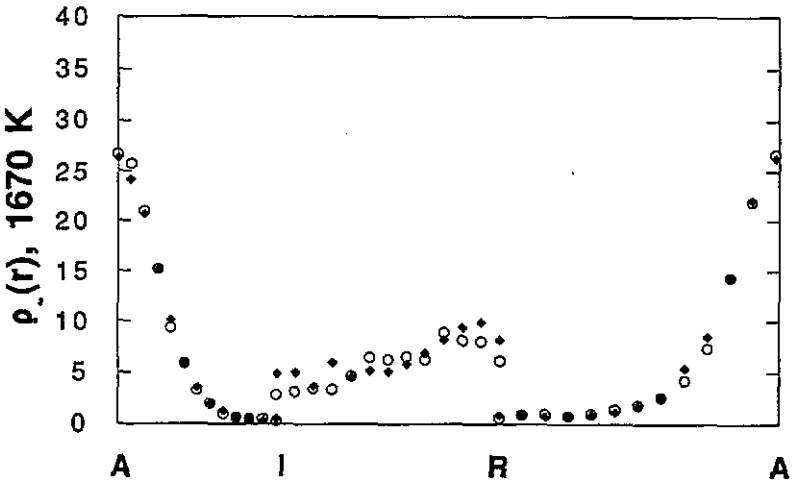

Figure 2. Single-particle probability distribution for F^- ions $\rho_-(r)$ calculated from the shell model (open circles) and the rigid-ion model (filled diamonds) for CaF_2 at 1670 K. The distribution is shown on lines of symmetry in the unit cell, passing from the anion regular site A ($\frac{1}{4}, \frac{1}{4}, \frac{1}{4}$), to the anion-cube-edge site I ($\frac{1}{4}, \frac{1}{4}, 0$), the anion-cube-centre site R ($\frac{1}{2}$, 0, 0), and back to A. Note the ten-fold magnification of scale in the region I–R.

Our results confirm the conclusions of previous work (e.g. Gillan 1989) that the anion distribution function is strongly concentrated on the regular anion sites all the way up to the melting point, in spite of the very high mobility of the anions at this temperature (see below). However, the distribution spreads out into a wide region

of the unit cell, reflecting the fact that the mobile ions take a range of paths as they jump between the regular sites. (For a detailed description of the diffusion process, see Gillan (1989).) The very close agreement between the rigid-ion and shell-model results for $\rho_-(r)$ is remarkable. Once again, the time-averaged structure in the superionic state seems to be unaffected by the inclusion of polarizability. We note in passing that the cation distribution (not shown here) confirms that the cations vibrate with larger amplitudes in the shell model.

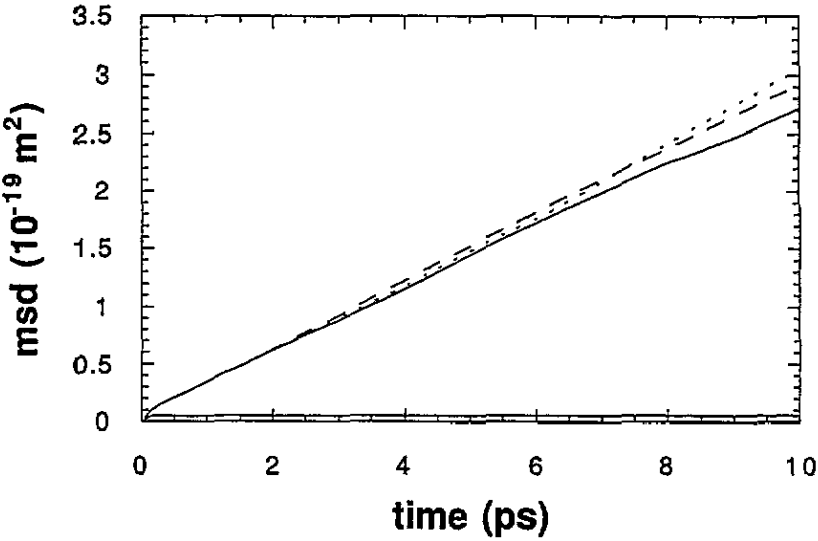

Figure 3. Time-dependent mean square displacement $\langle \Delta r_\alpha(t)^2 \rangle$ for cations and anions from shell-model simulations of CaF_2 at 1702 K. The three curves show results from three independent sections of a simulation run, each section having a duration of 12.5 ps.

4.3. Anion diffusion

We now turn to the dynamics of the ions. Figure 3 shows our shell-model results for the time-dependent mean square displacement $\langle \Delta r_\alpha(t)^2 \rangle$ for cations and anions at 1702 K. At all the four temperatures we have studied, the cation function tends to a constant value at long times, which shows that the cations do not diffuse. The anion function becomes asymptotically proportional to time, as expected for diffusing ions. From the slope, we obtain the anion diffusion coefficient D_-, according to the usual relation

$$\langle \Delta r_\alpha(t)^2 \rangle \rightarrow B_\alpha + 6D_\alpha|t| \qquad \text{as } |t| \rightarrow \infty. \tag{16}$$

The shell-model values for D_- obtained in this way are compared in figure 4 with earlier rigid-ion results (Gillan 1986) and with experimental values. The close agreement between rigid-ion and shell-model results shows that the explicit inclusion of polarizability has remarkably little quantitative effect on the diffusion dynamics in superionic CaF_2.

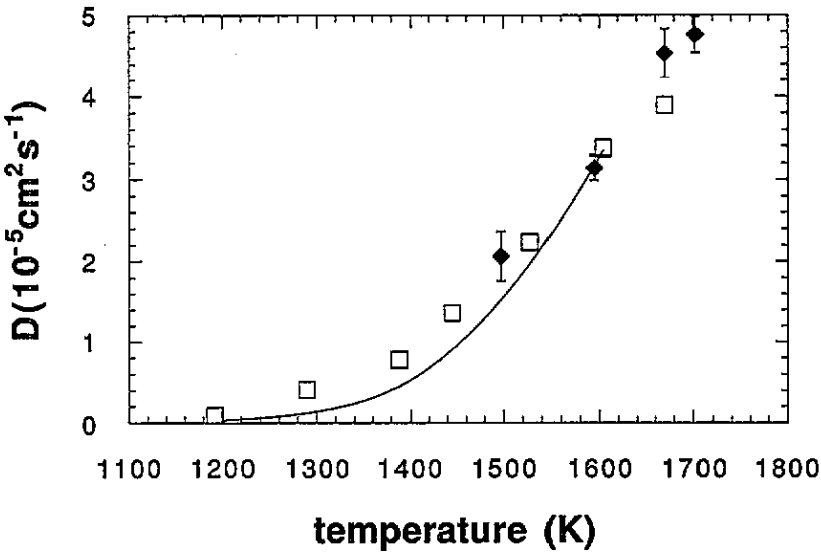

Figure 4. Simulation results for the anion diffusion coefficient D_- of CaF_2 using the shell-model (diamonds) and the rigid-ion model (squares) compared with experimental values (Derrington *et al* 1975) (curve).

5. Discussion

Two main results have been achieved in this work. Firstly, we have developed an improved method for performing shell-model MD simulation. Secondly, we have applied the method to study superionic behaviour in CaF_2.

The main feature of our simulation method is that it is based on conjugate-gradient relaxation rather than the steepest-descent technique used in earlier work. We expect this approach to give greater robustness and generality, and indeed the long simulations we have performed on a fairly large CaF_2 system confirm the stability of the method. The time step used is similar to those common in rigid-ion work. Although we are reporting here on the application of our code to CaF_2, we stress again that our aim has been to develop a general-purpose shell-model simulation program.

The general conclusion from our simulations of CaF_2 is that explicit inclusion of polarizability has a rather small effect on the quantities examined. This is, of course, an important conclusion, since it indicates that the many earlier MD studies of CaF_2 based on neglect of polarizability should be rather reliable. The conclusion is not unexpected, since neither Ca^{2+} nor F^- is a strongly polarizable ion. Even though the high-frequency dielectric constant ϵ_∞ of CaF_2 is 2.05, our comparison of rigid-ion and shell-model dispersion relations, mentioned in section 3, suggests that the rigid-ion description should be semiquantitatively correct.

We expect the situation to be very different for materials such as oxides containing the highly polarizable O^{2-} ion. We are currently applying shell-model MD to study ionic disorder and diffusion in the oxide superionic conductors UO_2 and Li_2O, and we hope to report on this work in the near future.

Acknowledgments

The development of the code and the production runs were performed on the Cray XMP-48 at RAL under SERC grant GR/H49108 and on a Hewlett–Packard 730 workstation financed by SERC grant GR/H31783. PJDL is supported by an SERC CASE studentship with AEA Technology; funding for this studentship from the Health and Safety Executive is gratefully acknowledged.

Note added in proof. Since the paper was submitted, the shell model MD code has been considerably refined. The removal of a small inconsistency between energy and forces has almost entirely eliminated the energy drift discussed in section 2.3.

References

Board J A and Elliott R J 1989 *J. Phys.: Condens. Matter* **1** 2427
Brass A 1989 *Phil. Mag.* A **59** 843
Catlow C R A and Mackrodt W C (ed) 1982 *Computer Simulation of Solids* (Berlin: Springer)
Catlow C R A and Norgett M J 1973 *J. Phys. C: Solid State Phys.* **6** 1325
Derrington C E, Lindner A and O'Keeffe M 1975 *J. Solid State Chem.* **15** 171
Dick B G and Overhauser A W 1958 *Phys. Rev.* **112** 90
Dixon M and Gillan M J 1978 *J. Phys. C: Solid State Phys.* **11** L165
Dixon M and Gillan M J 1980 *J. Physique* **41** C6–24
Elcombe M M and Pryor A W 1970 *J. Phys. C: Solid State Phys.* **3** 492
Evangelakis G A and Pontikis V 1989 *Europhys. Lett.* **8** 599
Evangelakis G A and Pontikis V 1991 *Phys. Rev.* B **43** 3180
Fletcher R 1980 *Practical Methods of Optimization* vol 1 (New York: Wiley) p 63
Gillan M J 1986 *J. Phys. C: Solid State Phys.* **19** 3391
Gillan M J 1989 *Ionic Solids at High Temperatures* ed A M Stoneham (Singapore: World Scientific) p 169
Harding J H 1989 *Ionic Solids at High Temperatures* ed A M Stoneham (Singapore: World Scientific) p 121
Harding J H 1990 *Rep. Prog. Phys.* **53** 1403
Hayes W and Hutchings M T 1989 *Ionic Solids at High Temperatures* ed A M Stoneham (Singapore: World Scientific) p 247
Jacucci G, McDonald I R and Rahman A 1976 *Phys. Rev.* A **13** 1581
Lindan P J D and Gillan M J 1991 *J. Phys.: Condens. Matter* **3** 3929
O'Sullivan K F and Madden P A 1991 *J. Phys.: Condens. Matter* **3** 8751
Parrinello M, Rahman A and Vashishta P 1983 *Phys. Rev. Lett.* **50** 1073
Press W H, Flannery B P, Teukolsky S A and Vetterling W T 1986 *Numerical Recipes* (Cambridge: Cambridge University Press) ch 10
Rahman A 1976 *J. Chem. Phys.* **65** 4845
Sangster M J and Dixon M 1976 *Adv. Phys.* **25** 247
Smith W and Gillan M J 1992 *J. Phys.: Condens. Matter* **4** 3215
Walker A B, Dixon M and Gillan M J 1982 *J. Phys. C: Solid State Phys.* **15** 4061
Wolf M L, Walker J R and Catlow C R A 1984 *Solid State Ion.* **13** 33